Thrust and Performance Analysis of Rockets and Ramjets

Comparative CFD study of a ramjet, chemical rocket, and resistojet

AUTHOR	Om Manish Patel
COURSE	AESP 314 – Air-Breathing and Rocket Propulsion Technologies
INSTITUTION	University of South Carolina
INSTRUCTOR	Prof. Mostafa Mobli
SOFTWARE	ANSYS Fluent
DATE	December 1, 2025

Contents

1 Abstract

Three propulsion systems, a ramjet, a chemical rocket, and a resistojet, were analyzed numerically in ANSYS Fluent to compare the flow physics governing thrust generation across fundamentally different energy-addition mechanisms. Each engine was modeled with simplified two-dimensional geometry informed by classical propulsion literature and verified through a mesh-independence study spanning five grid densities.

The ramjet was simulated at three flight Mach numbers with methane and hydrogen fuels at two fuel-to-air ratios. The chemical rocket was evaluated across two propellants, two mixture ratios, and two chamber lengths. The resistojet was swept over inlet velocity, electric field strength, and nozzle diameter.

Ramjet performance is dominated by flight Mach number and fuel choice: hydrogen at Mach 3 produced the highest thrust (122 kN) and the highest fuel-specific impulse (2,492 s). Chemical rocket results depend strongly on chamber length and mixture ratio, with lean hydrogen in a long chamber giving the best balance. Resistojet trends confirm that electrical power input, not mass flow, is the primary driver of specific impulse. Across all three, the study demonstrates how geometry, energy-addition mechanism, and operating condition jointly determine engine performance.

1.1 Notes on this revision

This revision is typeset from the original submission and from its source workbook. **No recorded value has been altered.** Where a tabulated quantity does not close against the equation that defines it, the discrepancy is documented with the arithmetic shown and flagged for re-post-processing, rather than adjusted.

Four changes were made to the presentation, and two claims made in an intermediate typeset version are withdrawn.

1. **Resistojet table columns restored.** The source table carries seven data columns: exit area, throat area, heater volume, inlet mass flow, and outlet mass flow. An intermediate version mapped heater volume into the throat-area column, dropped the actual throat area and the chamber-pressure column, and collapsed inlet and outlet mass flow into a single figure. All seven columns are restored in Tables 6 and 7. A claim in that version that "throat area exceeds exit area" was computed on heater volume and is withdrawn; the area comparison is revisited correctly in Section 6.2.
2. **Thrust coefficient is computable.** That version stated that C_F could not be evaluated because throat area was not recorded for the rocket cases. This is wrong: `propprojfr.xlsx` records exit area and throat area for every case. C_F is evaluated in Section 5.1. TSFC remains genuinely uncomputable, since only total mass flow was logged and Equation 3 needs fuel-only mass flow.
3. **Specific impulse definition stated.** The ramjet I_{sp} values are *fuel-specific* impulse, computed on fuel mass flow only, which is the standard airbreathing convention. This is now stated explicitly in Section 3.4, because the values are otherwise easy to misread against rocket I_{sp}.
4. **Rocket mixture ratio terminology.** The chemical rocket section described its mixture parameter as a "fuel-to-air ratio." A rocket carries no air; the parameter is a fuel-to-oxidizer ratio and

is relabeled F/O throughout Section 5.

Internal consistency checks are added in Sections 4.1, 5.1, and 6.2. All contour output is reproduced: one representative case per engine in the main body, and every remaining case in Appendix A.

2 Introduction

The objective of this project is to analyze and compare three propulsion systems that generate thrust by different physical mechanisms but share a common requirement: accelerating a working fluid. Modeling all three within one framework permits a consistent comparison that studying any one in isolation would not.

The investigation has three parts:

- **Ramjet.** Airbreathing supersonic propulsion. Examines how flight Mach number, fuel type, and fuel-to-air ratio affect combustion behavior and thrust.
- **Chemical rocket.** Closed-system propulsion with onboard fuel and oxidizer. Quantifies how propellant selection and chamber geometry drive thrust, specific impulse, and thrust coefficient.
- **Resistojet.** Electric propulsion in which thermal rather than chemical energy expands the working fluid. Evaluates how energy addition influences exhaust conditions.

2.1 Ramjet background

Ramjets rely on vehicle forward motion to compress incoming air before combustion, eliminating rotating compressors entirely. This architecture produces efficient thrust at supersonic speeds, particularly between Mach 2 and 4, where inlet shock systems decelerate the flow to subsonic conditions for fuel injection and burning. Historical reviews of U.S. Navy ramjet development show that both liquid- and solid-fueled ramjets sustained long-range, high-speed flight using lightweight engines with few moving parts [1].

Modern research emphasizes the flow physics governing performance. Inlet–combustor interactions strongly influence pressure recovery, shock structure, thermal choking, and engine stability. Analytical work has shown that ramjets exhibit distinct operational modes, ramjet mode, scramjet mode, and inlet unstart, each defined by characteristic shock configurations and combustion-induced pressure responses [2]. These transitions depend sensitively on geometry, heat release, and incoming Mach number, and can produce hysteresis that complicates engine control.

This classification explains why small changes in fueling or back pressure force abrupt transitions between stable and unstable operation, and it establishes why accurately capturing inlet–combustor coupling determines the reliability of any numerical thrust prediction.

2.2 Chemical rocket background

Chemical rockets store both fuel and oxidizer onboard, allowing combustion independent of the surrounding atmosphere and enabling operation from ground launch through vacuum. The core components are a pressurized combustion chamber, an injector system, and a convergent–divergent nozzle that converts chemical energy into high-velocity exhaust. Chamber pressure, mixture ratio, and nozzle expansion geometry together govern exhaust velocity and specific impulse [3].

Performance depends on the thermochemical properties of the propellant pair and on the efficiency of energy conversion inside the chamber. High-temperature, high-pressure combustion increases exhaust momentum, while an optimized nozzle maximizes the conversion of pressure into kinetic energy across the expansion region. Real-nozzle effects, including boundary layer losses, non-ideal expansion, and finite-rate chemistry, reduce performance relative to idealized predictions.

Unlike ramjets, which draw oxidizer and inlet compression from the atmosphere, chemical rockets must generate all pressure internally and carry all reactants. This places strong constraints on propellant mass flow, chamber geometry, and nozzle design.

2.3 Resistojet background

Resistojets produce thrust by electrically heating a stored propellant and expanding it through a nozzle. Because they use no combustion, they are mechanically simple and lightweight, which suits small satellites where power is limited but reliability and compactness matter. Typical applications include attitude control, collision avoidance, and small orbital adjustments on CubeSats [4].

A resistojet consists of a heating element, a small warming chamber, and a convergent–divergent nozzle. Raising propellant temperature increases exhaust velocity, improving both thrust and specific impulse. Performance depends strongly on how effectively heat transfers into the propellant and how much is lost by radiation or conduction to the surrounding structure. Practical challenges include maintaining consistent heating, preventing material cracking, and achieving stable thrust output.

3 Modeling

3.1 Geometry

All three geometries were constructed in ANSYS DesignModeler as simplified two-dimensional representations of the internal flow path, sketching the inlet, combustion region, converging section, throat, and diverging nozzle. Proportions followed classical propulsion literature: liquid-propellant chamber and nozzle contours after Huzel and Huang [3], ramjet combustor and inlet layouts after Waltrup [1], and the heater–chamber–nozzle configuration after Vilenius [4].

Several design iterations were generated for each system, exploring different chamber lengths, nozzle expansion ratios, inlet configurations, and mixing approaches. Candidates were evaluated on mesh quality, mixing behavior, and numerical stability before a final geometry was selected. The rejected iterations are reproduced in Appendix A.

Named selections were assigned to the inlet, outlet, walls, and axis of symmetry. For the chemical rocket, the inlet boundary was divided into alternating fuel and oxidizer segments to produce immediate mixing within the chamber volume. This approximates the distributed mixing of a real injector while remaining tractable for a two-dimensional axisymmetric model.

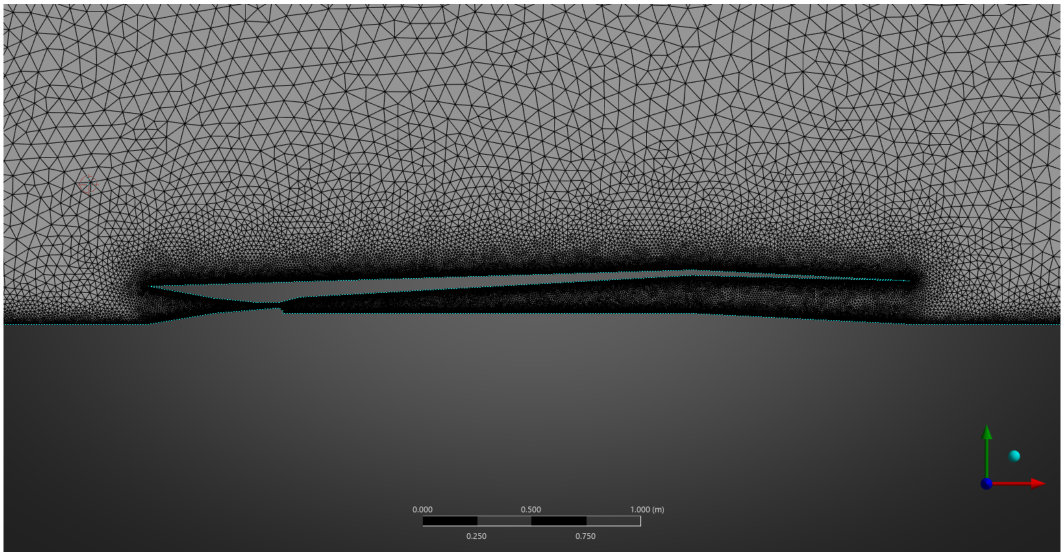

(a) Final ramjet geometry and mesh.

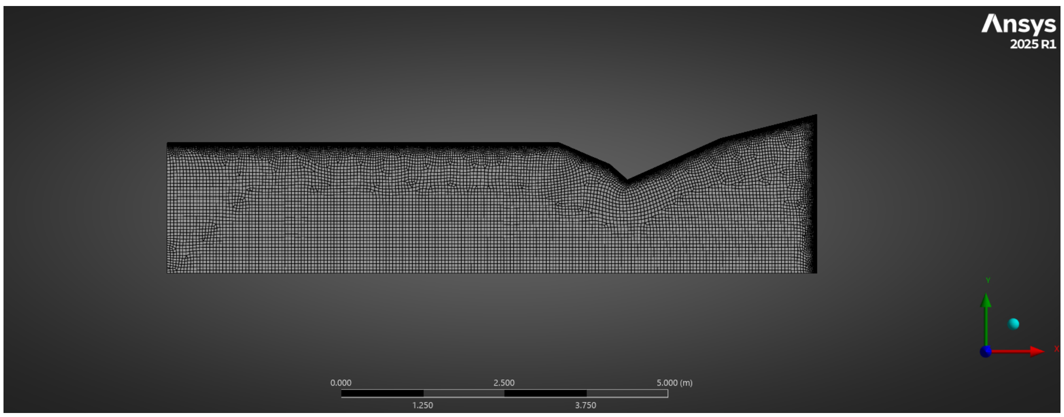

(b) Final chemical rocket geometry and mesh.

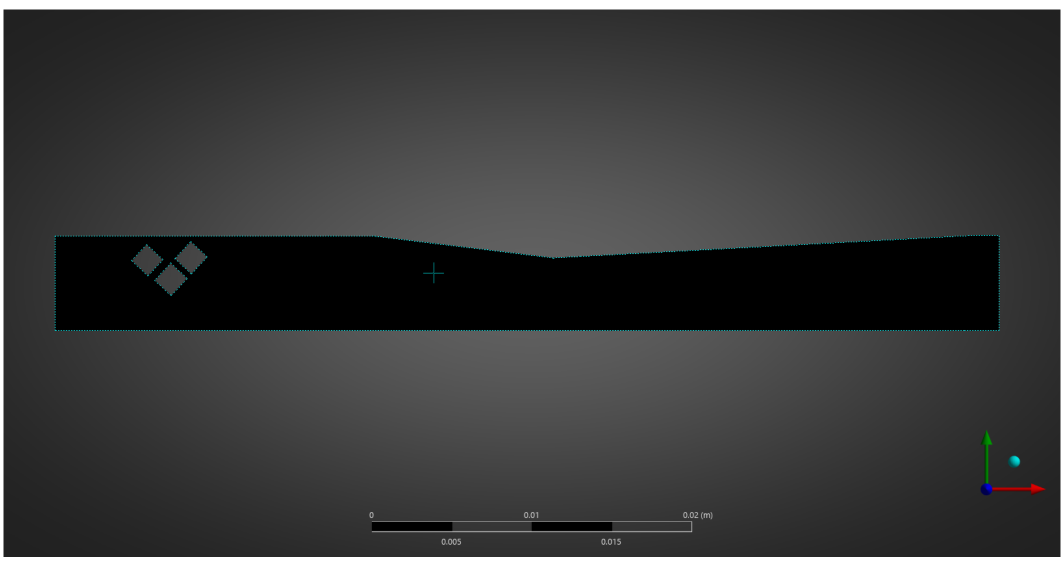

(c) Final resistojet geometry, with the heater elements visible upstream of the throat.

Figure 1. Selected geometries after iteration on mesh quality, mixing behavior, and numerical convergence.

3.2 Meshing and grid independence

Meshing used a fine grid with targeted refinement along the inlet boundaries, the alternating fuel–oxidizer injection segments, and particularly the throat, where choking and rapid acceleration produce steep gradients.

Five mesh densities, coarse, coarse-medium, medium, medium-fine, and fine, were generated for a grid-independence study, with exit velocity tracked as the convergence metric. The solution asymptotes above approximately 200,000 elements, and the difference between the medium-fine and fine meshes was small enough to accept the fine mesh as adequately resolved.

The study was performed on the ramjet configuration only, and its conclusion was applied to all three engines. That is a real limitation and is repeated in Section 7.

3.3 Solver configuration

The k–ω SST model was selected for its near-wall accuracy and stability in flows with strong pressure gradients, recirculation zones, and shock-adjacent regions, all characteristic of reactive propulsion devices.

Table 1. Solver settings.

Setting	Value
Solver	Pressure-based, steady
Energy equation	Enabled
Species transport	Enabled for reacting cases
Combustion model	Finite-Rate / Eddy-Dissipation
Turbulence model	k–ω SST

3.4 Performance relations

Fluent output was converted to engine performance metrics using the standard relations:

$$T = \dot{m}V_e + (p_e - p_a)A_e \tag{1}$$

$$I_{sp} = \frac{T}{\dot{m}g_0} \tag{2}$$

$$\mathrm{TSFC} = \frac{\dot{m}_{\mathrm{fuel}}}{T} \tag{3}$$

$$C_F = \frac{T}{p_c A_t} \tag{4}$$

with $g_0 = 9.806{,}65\,\mathrm{m/s^2}$. These are directly compatible with Fluent-reported quantities: mass flow rate, exit velocity, exit pressure, chamber pressure, and reaction rates.

Which mass flow enters I_{sp}. Equation 2 is evaluated with different mass flows for the two engine families, and the distinction matters for reading the results. For the **ramjet**, $\dot{m}$ is the fuel mass flow only, since the oxidizer is atmospheric and is not carried. This is the standard airbreathing convention and is why the tabulated ramjet values reach the thousands of seconds; they are not comparable to rocket I_{sp} and should not be read as such. For the **chemical rocket and resistojet**, $\dot{m}$ is the total propellant mass flow, since all mass is carried onboard.

4 Ramjet Results

The ramjet was evaluated at three Mach numbers with hydrogen and methane at fuel-to-air ratios of 5% and 20%.

Table 2. Ramjet performance across all five cases, as recorded. I_{sp} is fuel-specific impulse.

Case	Mach	Fuel	F/A	Thrust [N]	TSFC [kg/(N s)]	I_{sp} [s]
1	$1^{\dagger}$	H_2	0.05	28,422	1.26×10^{-4}	580
2	2.0	CH_4	0.20	54,835	3.85×10^{-4}	279
3	2.0	H_2	0.05	48,261	1.04×10^{-4}	984
4	3.0	CH_4	0.20	117,854	1.70×10^{-4}	601
5	3.0	H_2	0.05	122,211	4.03×10^{-5}	2,492

† **Case 1 Mach number is inconsistent in the source.** The table records Mach 1 while the surrounding text and the figure caption both describe Mach 1.5. The tabulated value is reproduced unchanged above. The discrepancy matters because a ramjet at Mach 1 has essentially no inlet compression and would not sustain the tabulated thrust, which argues for Mach 1.5 being correct, but the run log needed to settle it is not available. Both values should not be carried forward; the case should be re-identified from the solver session before Case 1 is cited.

4.1 Internal consistency of the tabulated metrics

TSFC and fuel-specific impulse are not independent. Combining Equations 2 and 3 with $\dot{m} = \dot{m}_{\text{fuel}}$ gives

$$\text{TSFC} = \frac{1}{I_{sp}\, g_0} \tag{5}$$

so the two tabulated columns must agree. Table 3 applies this test.

Table 3. Consistency check of TSFC against I_{sp} using Equation 5.

Case	TSFC recorded	$1/(I_{sp} g_0)$	Difference [%]	Status
1	1.26×10^{-4}	1.76×10^{-4}	28.4	Fails
2	3.85×10^{-4}	3.66×10^{-4}	5.3	Borderline
3	1.04×10^{-4}	1.04×10^{-4}	0.4	Closes
4	1.70×10^{-4}	1.70×10^{-4}	0.2	Closes
5	4.03×10^{-5}	4.09×10^{-5}	1.5	Closes

Cases 3, 4, and 5 close to better than 2%, which is rounding. Case 1 is off by 28%, meaning the fuel mass flow implied by its TSFC (3.6 kg/s) does not match the one implied by its I_{sp} (5.0 kg/s).

One of the two Case 1 entries was evaluated with a different mass flow than the other. The recorded values are left unaltered because the surface report needed to determine which is correct is not available; Case 1 should be re-post-processed before its TSFC is used quantitatively. Case 2 sits at 5%, borderline but plausible as accumulated rounding.

The headline result, Mach 3 hydrogen at 122 kN and 2,492 s, is unaffected: Case 5 passes the check to 1.5%.

4.2 Discussion

Ramjet thrust depends on inlet total-pressure recovery, heat addition during combustion, and the resulting exit momentum $\dot{m}V_e$ in Equation 1. As flight Mach number increases, the inlet compresses the flow more effectively, raising stagnation pressure and enabling the combustor to generate a larger pressure rise and higher exit velocity. This produces the sharp thrust increase from Mach 2 to Mach 3, where both the methane-rich and hydrogen cases exceed 117 kN.

Fuel type plays an equally strong role. Hydrogen, with low molecular weight and lighter combustion products, yields substantially higher specific impulse (up to 2,492 s) and lower TSFC than methane. This is consistent with classical ramjet thermodynamics, where I_{sp} scales with the square root of chamber temperature over molecular weight.

The contours confirm the mechanism. Hydrogen cases show nearly complete fuel burnout and a well-developed high-temperature core. Methane cases, particularly at 20% fuel-to-air ratio, show pockets of unburned fuel and cooler zones, direct evidence of incomplete combustion and the reason for their higher TSFC.

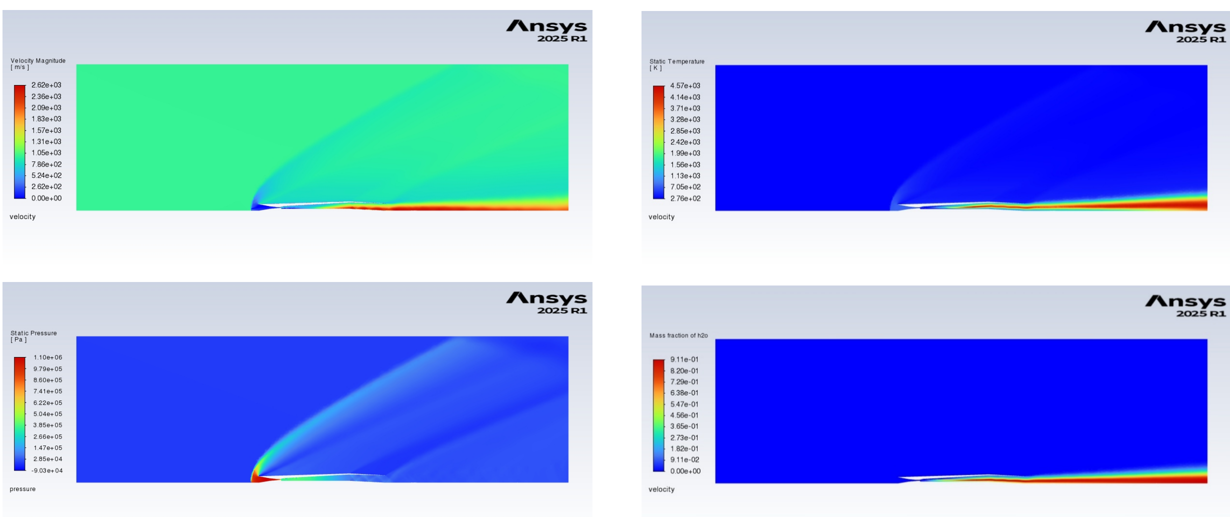

Figure 2. Ramjet Case 5 (Mach 3, hydrogen, F/A = 0.05), the best-performing case. Velocity magnitude, static temperature, static pressure, and fuel mass fraction, as exported. The high-temperature core forms downstream of the injection region and persists to the exit, and the fuel mass fraction field shows nearly complete burnout before the throat. Cases 1–4 appear in Appendix A.

4.3 Geometric sensitivities

Ramjet geometry controls residence time, mixing rate, shock behavior, combustion completeness, and expansion efficiency, all of which set final thrust and fuel efficiency. Combustor length governs how completely fuel and air mix and burn; injector layout sets turbulence scale and mixing rate; inlet geometry controls total-pressure recovery and shock structure; and nozzle expansion ratio determines whether exhaust momentum is maximized for the operating condition.

The results show three clear sensitivities:

1. **Incomplete methane combustion.** Methane cases at both Mach 2 and Mach 3 retain significant fuel mass fraction at the throat with uneven temperature contours, indicating the combustor is too short or mixing is insufficient.
2. **Excessive inlet shock losses at Mach 3.** Pressure contours show strong shock structures at the inlet lip, reducing available stagnation pressure and limiting downstream performance.
3. **Under-expanded exhaust.** Cases 2 and 4 show signs of under-expansion, suggesting the nozzle expansion ratio is not matched to the higher chamber pressures reached at those conditions.

Recommended changes. Lengthen the combustor or improve injector design for methane operation; refine the inlet lip and diffuser profile to reduce Mach 3 shock losses; and tune nozzle expansion ratio to the expected operating pressure. Each addresses a shortcoming visible directly in the flow-field results.

5 Chemical Rocket Results

The chemical rocket analysis covered two propellants (methane and hydrogen), two fuel-to-oxidizer ratios (0.05 and 0.20), and two chamber lengths (2 m and 5 m). All six cases share the same nozzle, with a recorded exit area of 19.47 and throat area of 6 in model units, an expansion ratio of $A_e/A_t = 3.25$.

Table 4. Chemical rocket performance, as recorded. I_{sp} computed from Equation 2 with total propellant mass flow.

Case	Fuel	F/O	L_c	$\dot{m}$ [kg/s]	V_e [m/s]	p_c [Pa]	T [N]	I_{sp} [s]
CR1	CH_4	0.05	5 m	105	966.0	934	101,430	98.5
CR2	CH_4	0.20	5 m	120	1,188.7	1,347	142,644	121.2
CR3	H_2	0.05	5 m	105	863.8	14,647	90,699	88.1
CR4	H_2	0.20	5 m	120	195.3	40,936	23,432	19.9
CR5	CH_4	0.05	2 m	105	974.0	545	102,420	99.5
CR6	H_2	0.05	2 m	105	465.0	175,746	48,825	47.4

TSFC remains uncomputable. Equation 3 requires the fuel-only mass flow, whereas only total mass flow was logged. This is recoverable by re-running with a species-resolved surface report at the inlet, and doing so is recommended before these results are used comparatively.

The pressure-thrust term was neglected. The tabulated thrust equals $\dot{m}V_e$ in every case, meaning Equation 1 was evaluated with $(p_e - p_a)A_e$ assumed zero. This is exact only at ideal expansion, and the low chamber pressures in several cases suggest the nozzles are not ideally expanded, so these thrust values carry an unquantified error.

5.1 Thrust coefficient

Because throat area and chamber pressure are both recorded, C_F can be evaluated from Equation 4. The result is a useful diagnostic rather than a performance figure.

Table 5. Thrust coefficient computed from the recorded chamber pressure and throat area. Physically realizable values for a chemical rocket lie between roughly 1.2 and 1.9.

Case	p_c [Pa]	A_t	C_F	Assessment
CR1	934	6	18.10	Non-physical
CR2	1,347	6	17.65	Non-physical
CR3	14,647	6	1.03	Plausible
CR4	40,936	6	0.10	Non-physical
CR5	545	6	31.32	Non-physical
CR6	175,746	6	0.05	Non-physical

Only CR3 produces a value anywhere near the physical range, and the spread across the set covers nearly three orders of magnitude. Since thrust and throat area are consistent between cases, the variable responsible is chamber pressure, which ranges from 545 Pa to 175,746 Pa across six cases of the same engine. A chamber pressure of 545 Pa is below atmospheric and cannot drive the tabulated 102 kN of thrust.

The most likely cause is that "chamber pressure" was read at inconsistent locations between cases, or that static rather than total pressure was reported in some of them. The recorded values are reproduced unchanged, and C_F should be regarded as unusable until chamber pressure is re-extracted at a defined plane with a consistent convention. This is the single highest-value fix available to this data set.

5.2 Discussion

Chamber length affects the two propellants differently. For methane, the longer chamber gives more complete combustion and higher exit velocity; the difference between CR1 and CR5 is modest because both are lean and already burn reasonably completely. Hydrogen shows a much larger effect: CR3 (5 m) reaches 864 m/s against 465 m/s for CR6 (2 m), nearly double.

Mixture ratio produces the clearest result in the set. Increasing the hydrogen fuel-to-oxidizer ratio from 0.05 to 0.20 collapses exit velocity from 864 to 195 m/s and drops I_{sp} from 88 to 20 s. This confirms the classical principle that raising mixture ratio increases thrust only while combustion remains near-stoichiometric; once the mixture goes fuel-rich, unburned propellant adds mass flow without adding energy, and specific impulse falls sharply.

Among all cases, lean hydrogen in a long chamber (CR3) gives the best balance of exit velocity and combustion completeness, while over-rich hydrogen (CR4) performs worst by a wide margin. CR3 is also the only case whose thrust coefficient lands in a physically plausible range, which is weak but consistent supporting evidence that it is the best-converged case in the set.

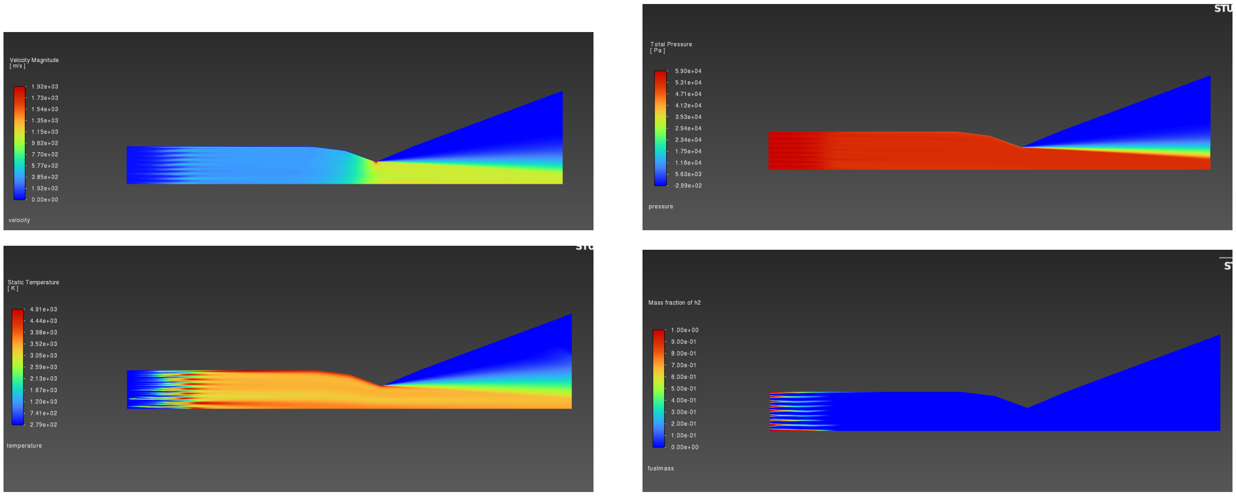

Figure 3. Chemical rocket Case CR3 (hydrogen, F/O = 0.05, 5 m chamber), the best-performing case. Velocity magnitude, total pressure, static temperature, and fuel mass fraction, as exported. Flow accelerates through the throat and expands in the diverging section; residual fuel mass fraction downstream of the throat indicates incomplete burnout. Cases CR1, CR2, and CR4–CR6 appear in Appendix A.

6 Resistojet Results

The resistojet cases examine the effect of inlet velocity, electric heating strength, and nozzle geometry on thruster performance. All quantities below are reproduced from the source table without modification.

Table 6. Resistojet geometry and mass flow, as recorded. Inlet and outlet mass flow are tabulated separately in the source and are kept separate here.

Case	V_{in} [m/s]	E-field [V/m]	Nozzle ∅ [mm]	A_e [m^2]	A_t [m^2]	Heater vol. [m^3]	$\dot{m}_{in}$	$\dot{m}_{out}$
R1	10	1.0×10^4	6	2.83×10^{-5}	0.005916	2.63×10^{-4}	0.069	0.069
R2	50	1.0×10^4	6	2.83×10^{-5}	0.005916	2.63×10^{-4}	0.384	0.385
R3	10	5.0×10^4	8	5.03×10^{-5}	0.005916	2.79×10^{-4}	0.069	0.077
R4	50	5.0×10^4	8	5.03×10^{-5}	0.005916	2.79×10^{-4}	0.376	0.375

Table 7. Resistojet performance, as recorded. Dashes mark entries left blank in the source.

Case	V_e [m/s]	p_e [Pa]	p_c [Pa]	T [N]	TSFC	I_{sp} [s]
R1	10.176	−0.051	12.322	0.013	5.695	0.018
R2	54.981	−0.169	−0.169	1.198	0.200	0.509
R3	10.995	−0.003	—	0.077	0.911	0.120
R4	54.640	0.000	—	1.745	0.215	0.473

6.1 Discussion

The resistojet behaves differently from the chemical systems because its thrust originates in electrical heating rather than combustion. Two trends emerge clearly:

- **Inlet velocity drives mass flow and thrust.** Raising inlet velocity from 10 to 50 m/s increases mass flow roughly fivefold and thrust by roughly two orders of magnitude in the R1→R2 comparison.
- **Electric field drives specific impulse.** Stronger fields raise heater power and exit temperature, increasing exhaust velocity. Comparing R1 and R3 at matched inlet velocity, increasing the field fivefold raises I_{sp} from 0.018 to 0.120 s.

The physical implication is that electrical energy input, not propellant throughput, governs efficiency. Increasing mass flow at fixed power dilutes the available energy per unit mass and reduces I_{sp}, which is why R2 and R4 have similar specific impulse despite different field strengths. This agrees with modern resistojet design practice, which emphasizes balancing electrical input against propellant mass flow.

6.2 Consistency of the resistojet tabulation

Three problems are visible in the tables above, and the trends should be read with them in mind.

1. Case R3 does not conserve mass. Inlet and outlet mass flow differ by 0.008 kg/s on 0.069 kg/s, an imbalance of 11.6%. The other three cases close to better than 0.3%. A steady-state solution must conserve mass, so R3 is not converged, and every quantity derived from it, including the I_{sp} value used in the electric-field comparison above, inherits that error. The field-strength trend is supported by R2 against R4 as well, so the conclusion survives, but R3 should be re-run.

2. Thrust does not equal $\dot{m}V_e$. Taking R1, $\dot{m}V_e = (0.069)(10.176) = 0.70\,\mathrm{N}$, against a recorded thrust of 0.013 N. The ratio between the two is not constant across cases (approximately 54, 18, 11, and 12 for R1 through R4), so this is not a single unit or scaling error. By contrast the chemical rocket table satisfies $T = \dot{m}V_e$ exactly in every case.

3. Throat area exceeds exit area. The recorded $A_t = 5.92 \times 10^{-3}\,\mathrm{m}^2$ is roughly two orders of magnitude larger than A_e, which is geometrically impossible for a convergent–divergent nozzle. A_e matches $\pi d^2/4$ for the stated nozzle diameter exactly, so the exit values are right and the throat value was extracted under a different convention, most likely a revolved rather than a planar area. It is also identical across all four cases despite two different nozzle diameters, which supports that reading.

Together these point to post-processing rather than to the solution itself, and all three are fixed by re-running with explicitly defined surface reports at the throat and exit planes. Until that is done the resistojet *trends* stand but the absolute magnitudes should not be quoted.

On the magnitude of these results. The absolute I_{sp} values are far below the several-hundred-second range typical of real resistojets, and the small negative exit pressures indicate the nozzle is operating well outside its design condition. These cases should be read as demonstrating parametric trends rather than as predicting achievable performance. A physically representative resistojet model would require a properly sized micro-nozzle, a resolved heater energy deposition model, and validation against measured thruster data.

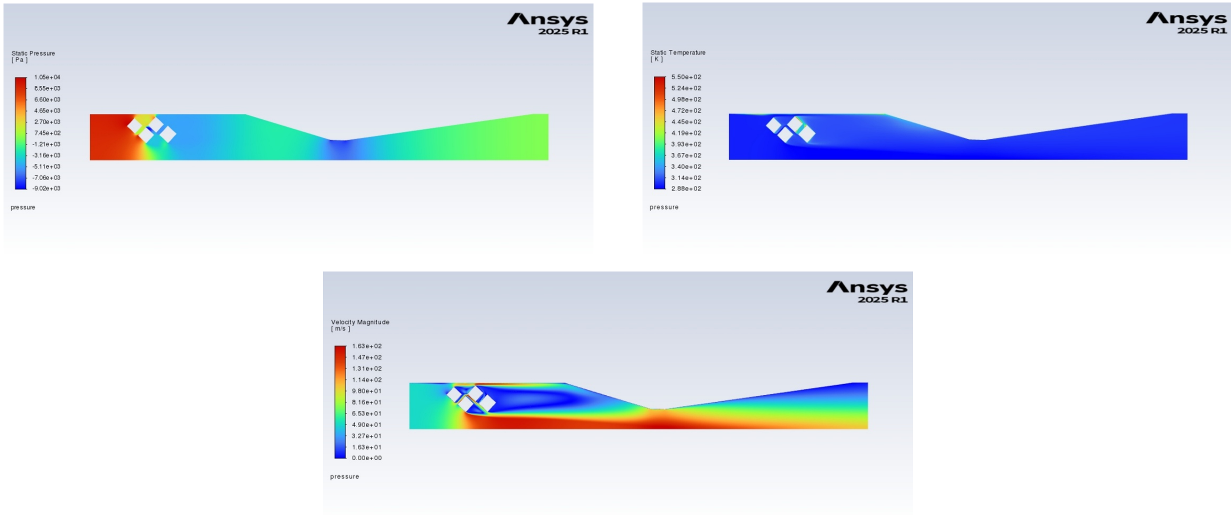

Figure 4. Resistojet Case R4 (50 m/s inlet, 5.0×10^4 V/m, 8 mm nozzle), the highest-thrust case. Static pressure, static temperature, and velocity magnitude, as exported. Heating occurs in the chamber upstream of the throat, with the temperature rise concentrated near the heater elements. Cases R1–R3 appear in Appendix A.

7 Limitations

1. **Two-dimensional simplification.** All three engines were modeled in 2D. Real injector mixing, swirl, and combustion instability are three-dimensional and cannot be captured.
2. **Pressure-thrust term neglected.** Tabulated thrust equals $\dot{m}V_e$ throughout, which is exact only under ideal expansion. Several cases show evidence of non-ideal expansion, so thrust carries unquantified error.
3. **Chamber pressure extraction.** The thrust coefficients in Section 5.1 span three orders of magnitude across six cases of the same engine, which localizes the problem to the recorded chamber pressure rather than to thrust or geometry.
4. **Incomplete performance logging.** Fuel-only mass flow was not recorded for the rocket cases, preventing computation of TSFC.
5. **Unconverged and inconsistent cases.** Ramjet Case 1 (Section 4.1) and resistojet Case R3 (Section 6.2) both fail internal checks and should be re-run.
6. **Combustion model.** The Finite-Rate/Eddy-Dissipation model assumes mixing-limited combustion and does not resolve detailed chemical kinetics. Predictions of incomplete combustion are qualitatively correct but not quantitatively reliable.
7. **Grid independence scope.** The mesh study was performed on the ramjet configuration only and its conclusion applied to all cases. Strictly, it should be repeated for each geometry.
8. **No experimental validation.** Results were compared against classical theory and published trends but not against measured engine data.

8 Conclusions

This project analyzed three propulsion systems in ANSYS Fluent, modeling compressible reacting and non-reacting flow across a range of operating conditions, and evaluated how inlet conditions, mixture ratios, geometry, and energy-addition mechanism affect performance.

Ramjet. Flight Mach number is the strongest driver of thrust, and hydrogen is the more efficient propellant due to low molecular weight and rapid reaction chemistry. Peak thrust (122 kN) and peak fuel-specific impulse (2,492 s) both occurred in the Mach 3 hydrogen case with a lean mixture, and that case passes its internal consistency check. Methane cases showed incomplete mixing at high fuel-to-air ratio, indicating that combustor length and injector configuration should be revised for better burnout and lower TSFC.

Chemical rocket. Performance depends strongly on chamber length, fuel type, and mixture ratio. Longer chambers improved methane combustion and exit velocity. Hydrogen performed well under lean conditions but collapsed when run fuel-rich, confirming that raising mixture ratio increases thrust only until combustion becomes fuel-rich. Lean hydrogen with a 5 m chamber gave the best overall balance and was the only case with a physically plausible thrust coefficient.

Resistojet. Thrust originates in electrical heating rather than chemical energy. Higher inlet velocity increased mass flow and thrust; stronger electric fields increased heater power, exit temperature, and exhaust velocity. Performance was modest compared to chemical propulsion, as expected, and the trends demonstrate that electrical input governs efficiency while added mass flow dilutes energy per unit mass. The absolute magnitudes are not usable as recorded.

Overall. Each system has a distinct optimal regime: ramjets favor high Mach number and lightweight fuels; chemical rockets favor matched chamber length and lean hydrogen mixtures; resistojets require coordination between inlet flow rate and heater power. The simulations also localized where each geometry should be refined, ramjet inlets for pressure recovery, methane combustors for mixing, and resistojet nozzles for expansion matching, demonstrating the value of CFD as a diagnostic as well as a predictive tool.

8.1 Highest-value next steps

One fix outranks the rest. Chamber pressure should be re-extracted at a single defined plane using a consistent convention across all six rocket cases. As Section 5.1 shows, that one quantity is responsible for thrust coefficients spanning three orders of magnitude on the same engine, and it is the largest single defect in the data set. Everything downstream of it is currently unusable.

Beyond that, every case should be re-run with surface reports defined explicitly at the throat and exit planes and with fuel-only mass flow logged separately from the total. That single change to the run setup resolves the missing TSFC column for the rocket cases and the throat area inconsistency in the resistojet tables at the same time, since both stem from quantities being extracted after the fact rather than defined before the solve.

Two individual cases need re-running on their own merits. Ramjet Case 1 fails the TSFC consistency check by 28% and its Mach number is recorded inconsistently between the table and the surrounding text, so the solver session should be used to settle both. Resistojet Case R3 does not conserve mass and is therefore not converged, which undermines any quantity derived from it.

Finally, two modeling choices should be revisited. The pressure-thrust term in Equation 1 should be evaluated rather than assumed zero, with nozzle pressure ratio reported alongside thrust so that the ideal-expansion assumption can be checked instead of inherited. And the grid-independence study should be repeated on the rocket and resistojet geometries rather than transferring a conclusion reached on the ramjet, since the throat gradients that set the resolution requirement differ substantially between the three.

References

[1] Waltrup, P. J., White, M. E., Zarlingo, F., and Gravlin, E. S., "History of U.S. Navy Ramjet, Scramjet, and Mixed-Cycle Propulsion Development," *Journal of Propulsion and Power*, Vol. 18, No. 1, 2002.

[2] Cui, K., Gao, Z., Li, X., and Yu, X., "Classification of Combustor–Inlet Interactions for Airbreathing Ramjet Propulsion."

[3] Huzel, D. K., and Huang, D. H., *Design of Liquid Propellant Rocket Engines*, NASA SP-125, National Aeronautics and Space Administration, 1971.

[4] Vilenius, V., "Resistojet Thruster: Reliability, Thrust Consistency, and Manufacturability," Master's Thesis, Aalto University, 2024.

[5] Hall, N., "Ramjet Propulsion Basics," NASA Glenn Research Center, 2021.

[6] Hall, N., "Rocket Propulsion Basics," NASA Glenn Research Center, 2021.

A Complete Field Output

Every contour recorded for this study is reproduced here. The representative cases shown in the main body are not repeated. Each panel carries its own Fluent legend identifying the field and its range.

A.1 Geometry iterations

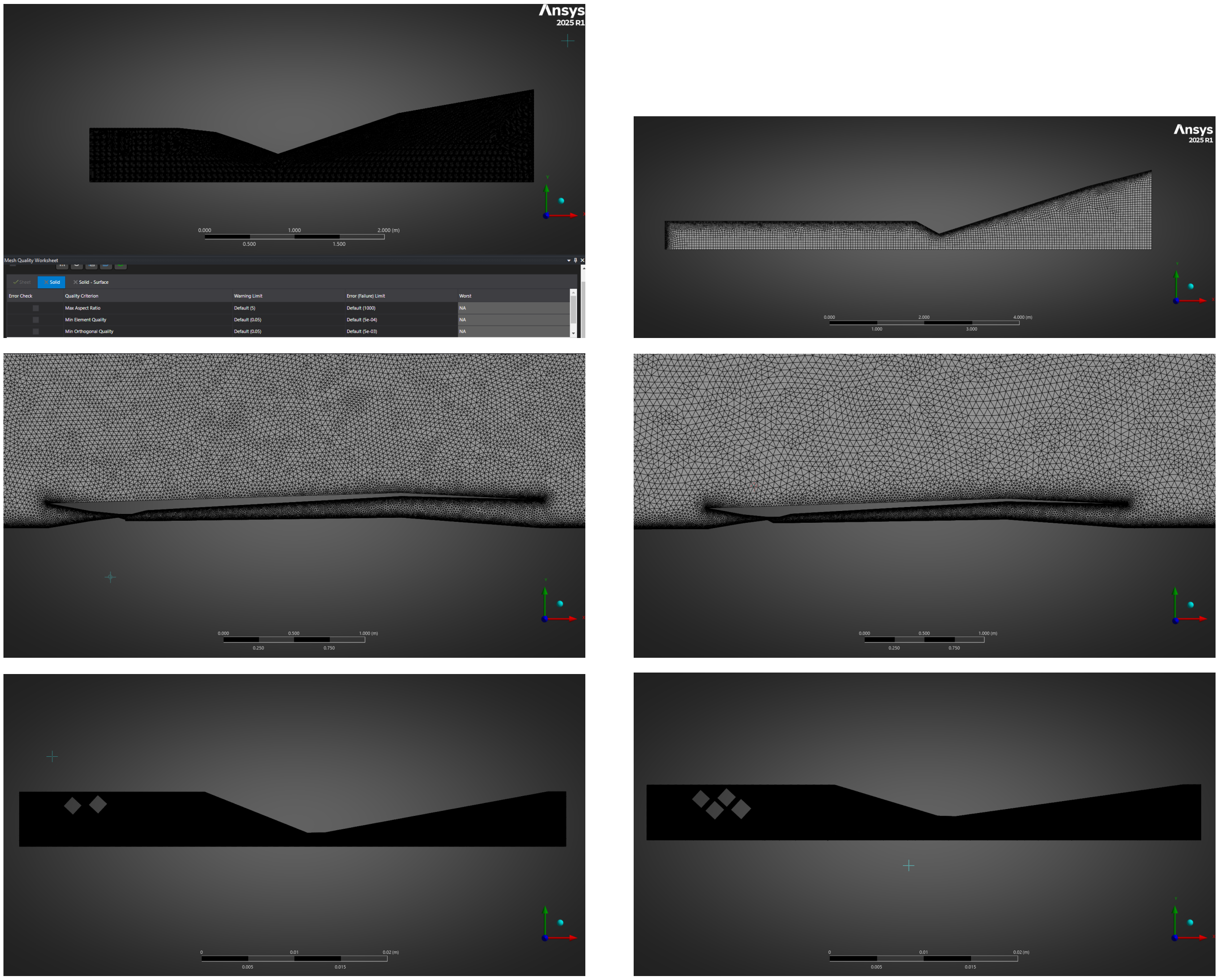

Figure 5. Candidate geometries and meshes generated during iteration, spanning the chemical rocket, ramjet, and resistojet flow paths. These were evaluated on mesh quality, mixing behavior, and numerical stability before the configurations in Figure 1 were selected.

A.2 Ramjet cases

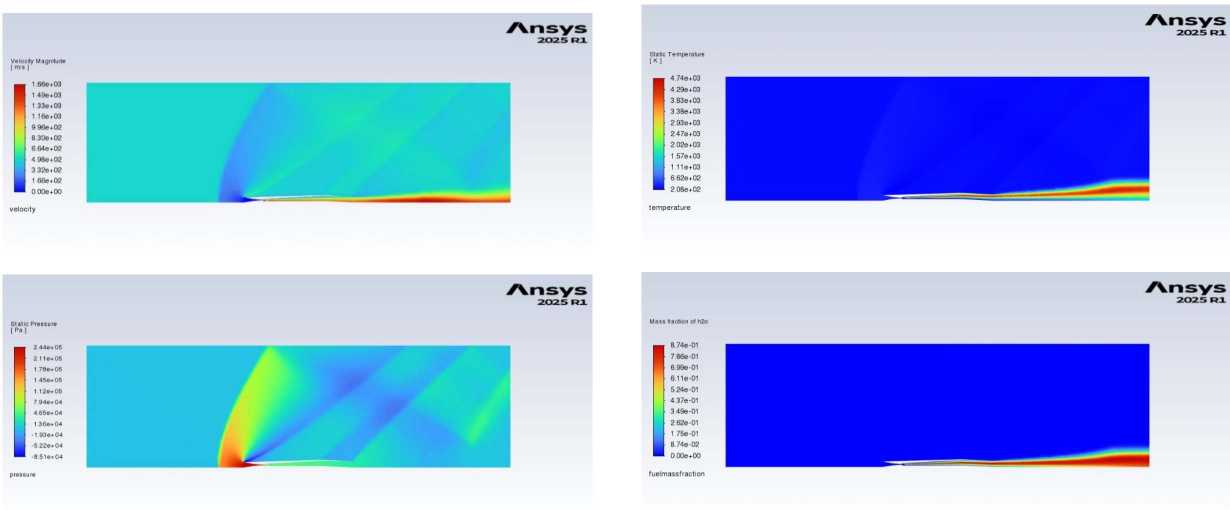

Figure 6. Ramjet Case 1 (Mach 1 (tabulated), hydrogen, F/A = 0.05). Velocity magnitude, static temperature, static pressure, and fuel mass fraction, as exported. Each panel carries its own Fluent legend.

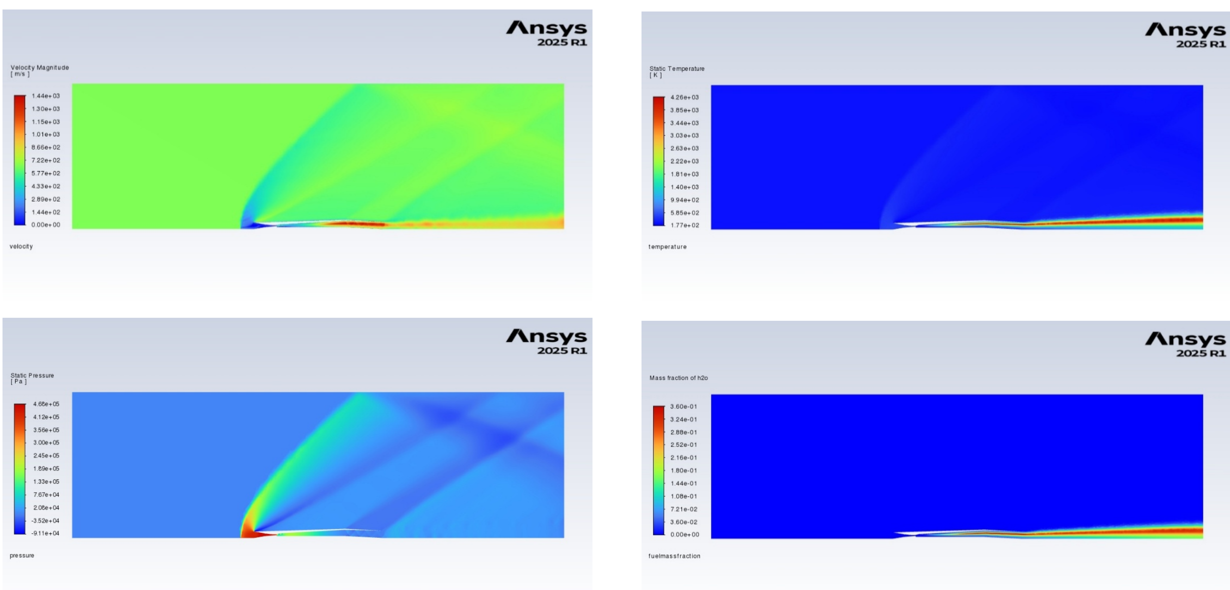

Figure 7. Ramjet Case 2 (Mach 2, methane, F/A = 0.20). Velocity magnitude, static temperature, static pressure, and fuel mass fraction, as exported. Each panel carries its own Fluent legend.

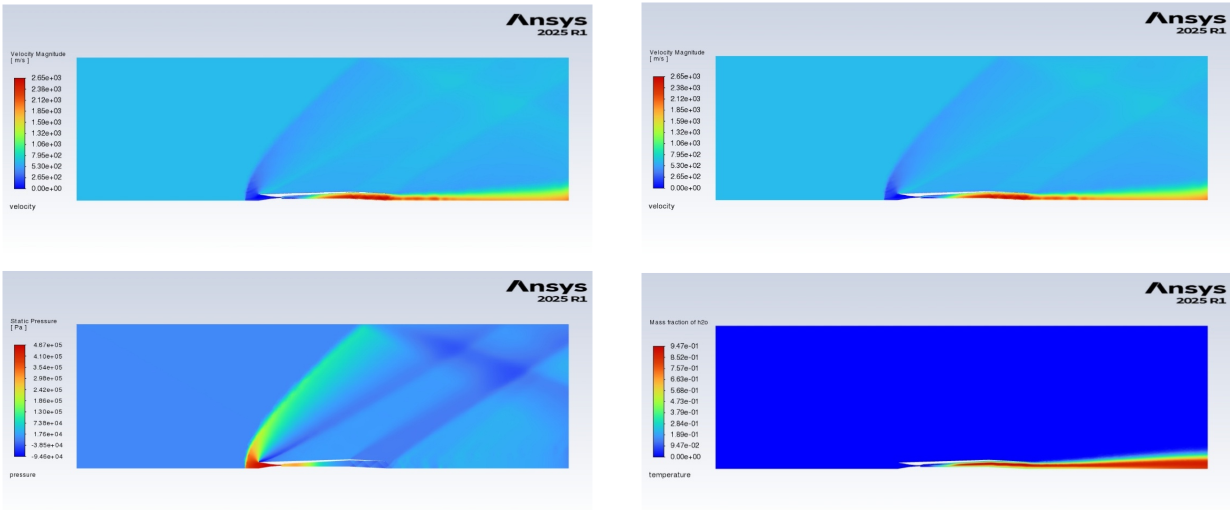

Figure 8. Ramjet Case 3 (Mach 2, hydrogen, F/A = 0.05). Velocity magnitude, static temperature, static pressure, and fuel mass fraction, as exported. Each panel carries its own Fluent legend.

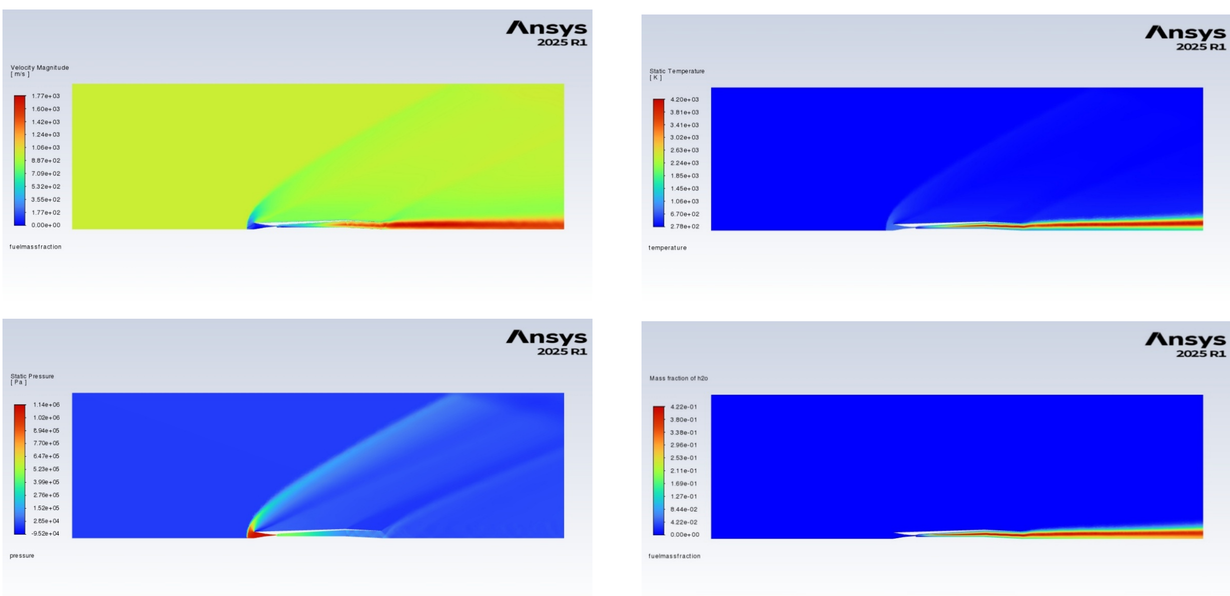

Figure 9. Ramjet Case 4 (Mach 3, methane, F/A = 0.20). Velocity magnitude, static temperature, static pressure, and fuel mass fraction, as exported. Each panel carries its own Fluent legend.

A.3 Chemical rocket cases

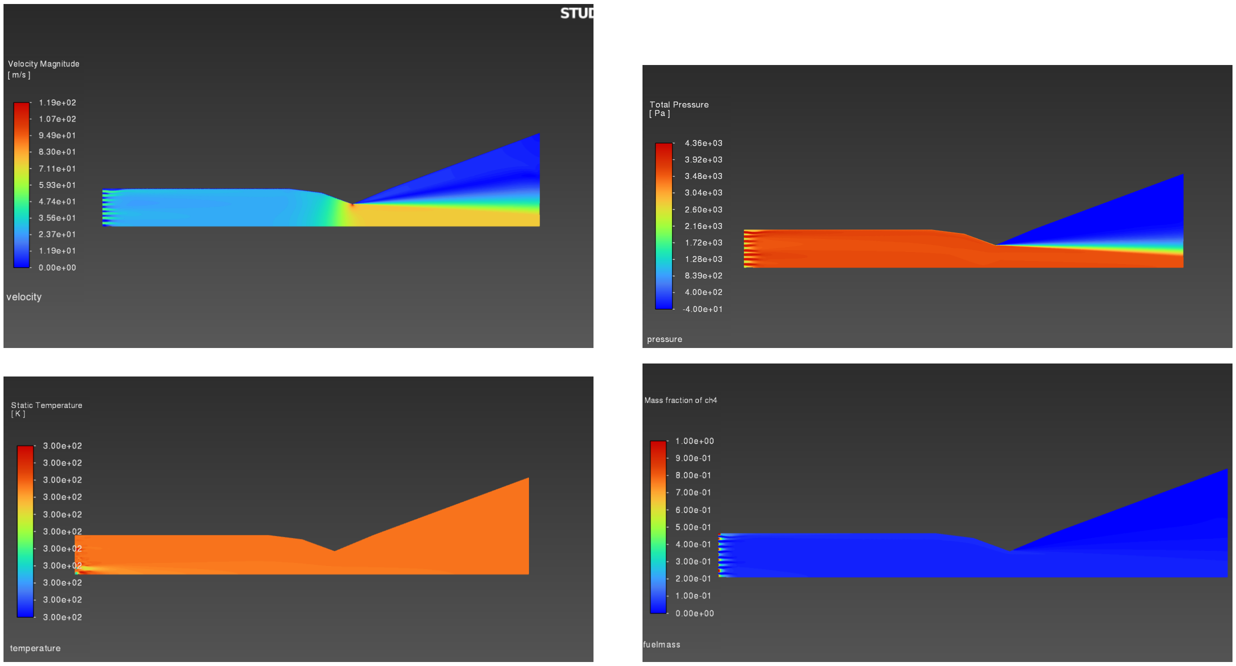

Figure 10. Chemical rocket Case CR1 (methane, F/O = 0.05, 5 m chamber). Velocity magnitude, total pressure, static temperature, and fuel mass fraction, as exported.

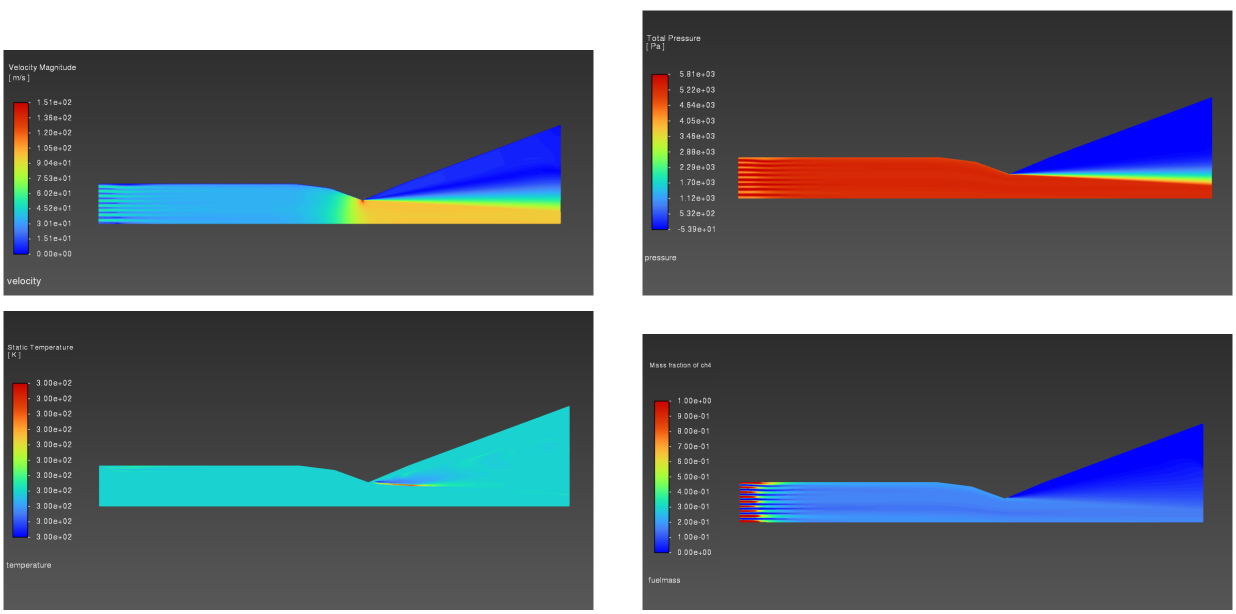

Figure 11. Chemical rocket Case CR2 (methane, F/O = 0.20, 5 m chamber). Velocity magnitude, total pressure, static temperature, and fuel mass fraction, as exported.

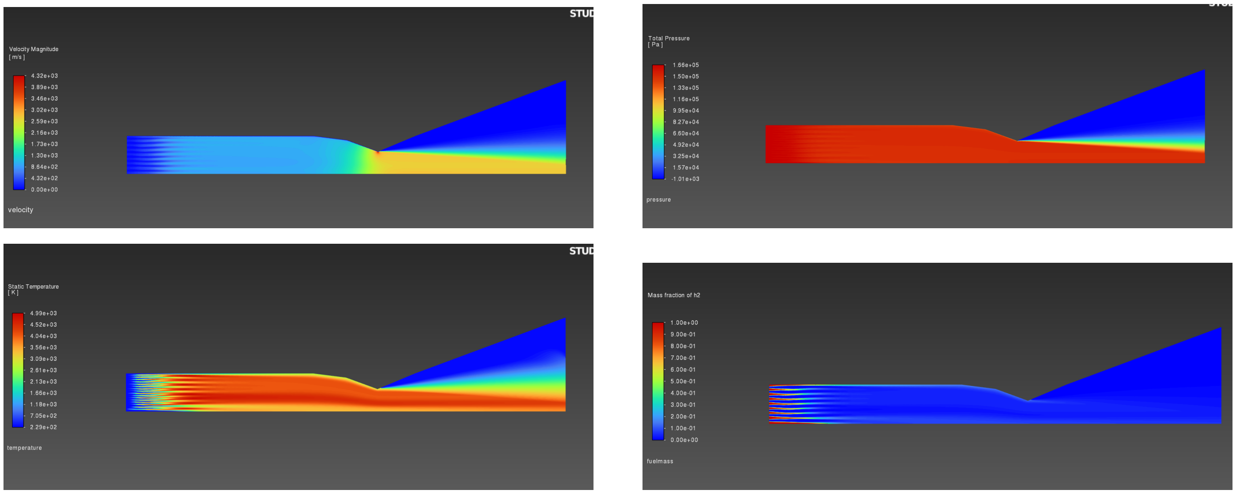

Figure 12. Chemical rocket Case CR4 (hydrogen, F/O = 0.20, 5 m chamber). Velocity magnitude, total pressure, static temperature, and fuel mass fraction, as exported.

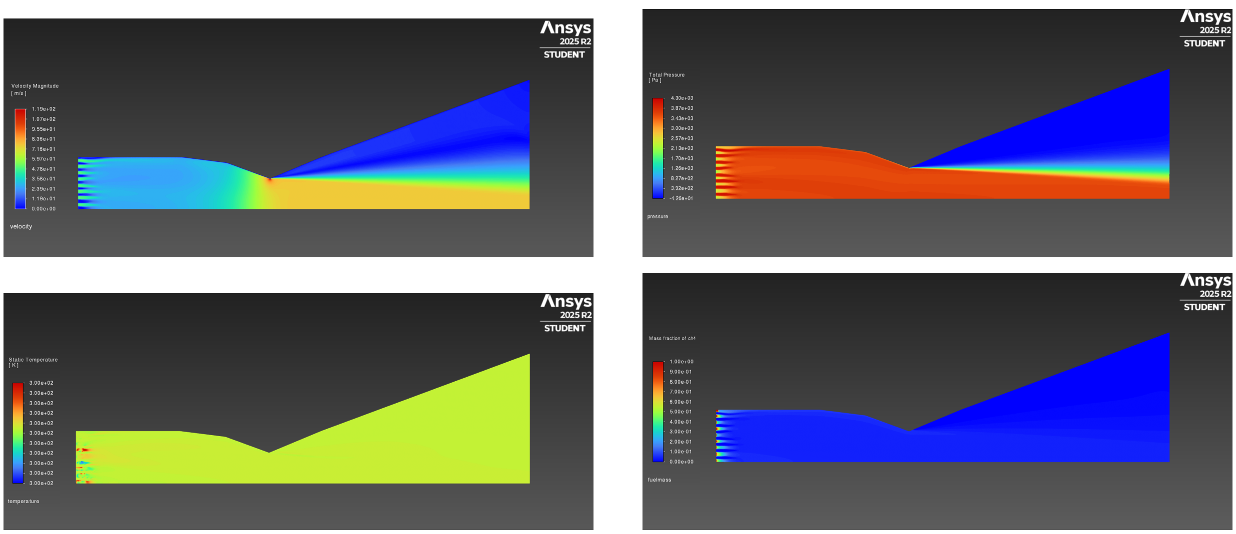

Figure 13. Chemical rocket Case CR5 (methane, F/O = 0.05, 2 m chamber). Velocity magnitude, total pressure, static temperature, and fuel mass fraction, as exported.

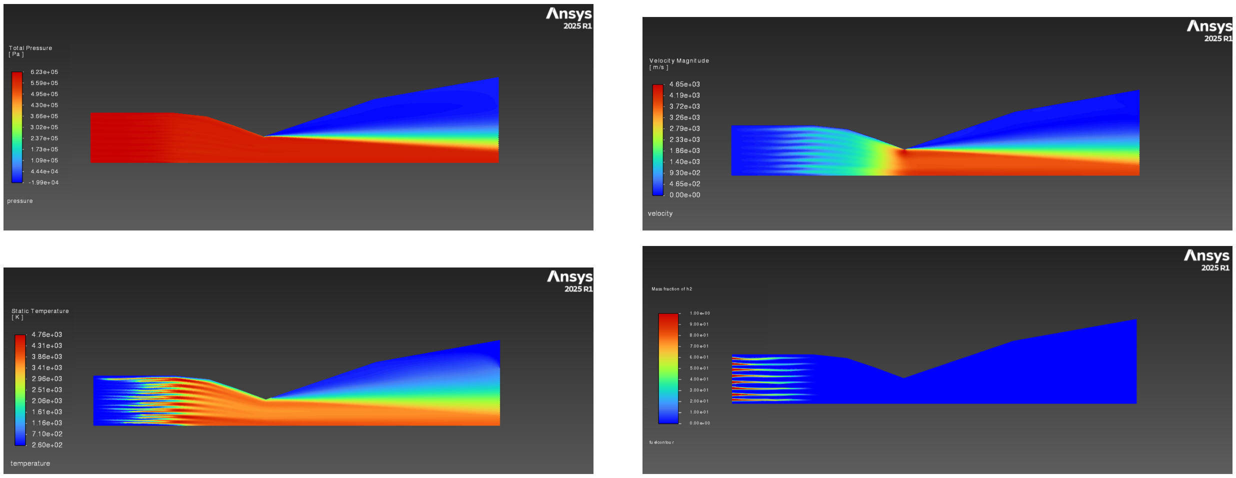

Figure 14. Chemical rocket Case CR6 (hydrogen, F/O = 0.05, 2 m chamber). Velocity magnitude, total pressure, static temperature, and fuel mass fraction, as exported.

A.4 Resistojet cases

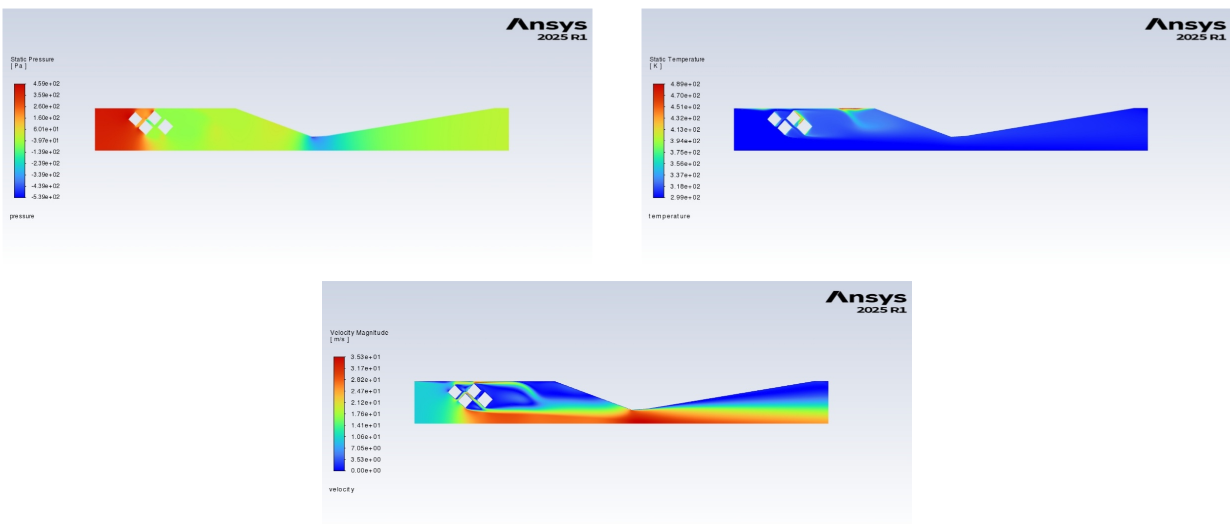

Figure 15. Resistojet Case R1 (10 m/s inlet, 1.0×10^4 V/m, 6 mm nozzle). Static pressure, static temperature, and velocity magnitude, as exported.

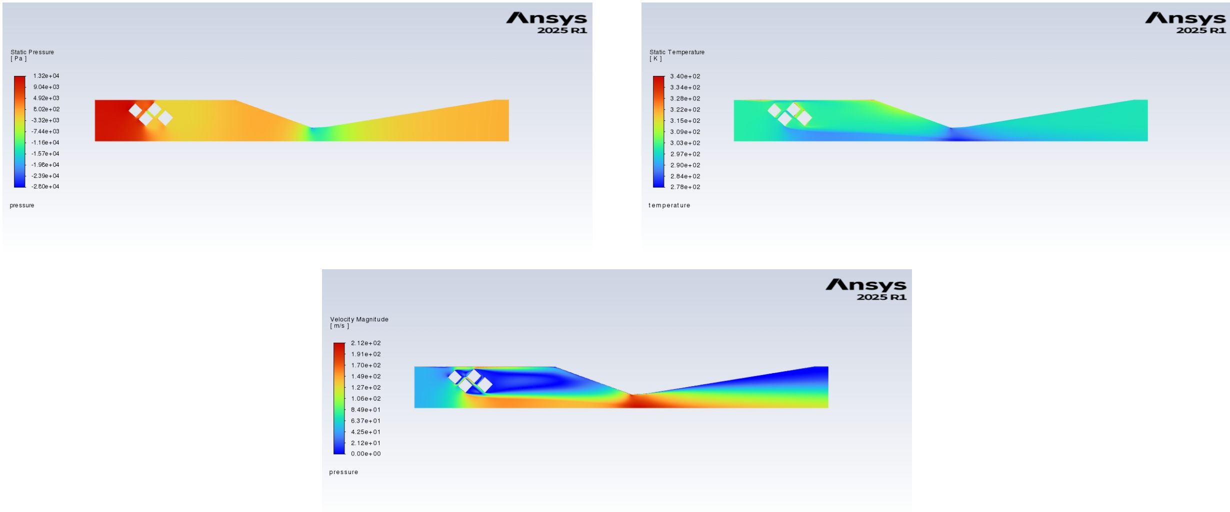

Figure 16. Resistojet Case R2 (50 m/s inlet, 1.0×10^4 V/m, 6 mm nozzle). Static pressure, static temperature, and velocity magnitude, as exported.

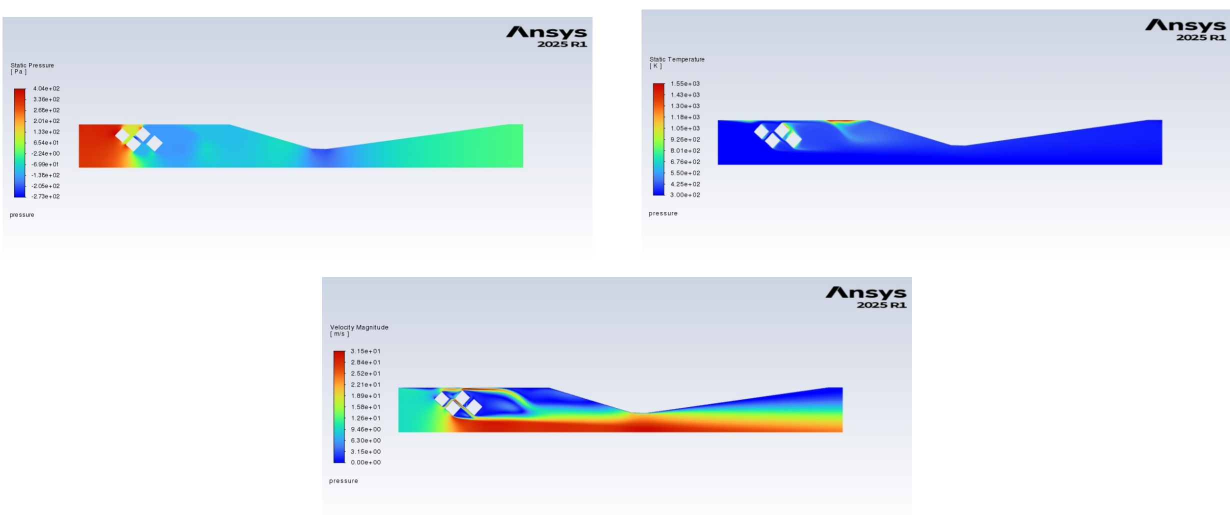

Figure 17. Resistojet Case R3 (10 m/s inlet, 5.0×10^4 V/m, 8 mm nozzle). Static pressure, static temperature, and velocity magnitude, as exported.